

An Influence-Receptivity Model for Topic based Information Cascades

Ming Yu, Varun Gupta, and Mladen Kolar

University of Chicago Booth School of Business

Abstract

We consider the problem of estimating the latent structure of a social network based on observational data on information diffusion processes, or *cascades*. Here for a given cascade, we only observe the time a node/agent is infected but not the source of infection. Existing literature has focused on estimating network diffusion matrix without any underlying assumptions on the structure of the network. We propose a novel model for inferring network diffusion matrix based on the intuition that an information datum is more likely to propagate among two nodes if they are interested in similar topics, which are common with the information. In particular, our model endows each node with an influence vector (how authoritative they are on each topic) and a receptivity vector (how susceptible they are on each topic). We show how this node-topic structure can be estimated from observed cascades. The estimated model can be used to build recommendation system based on the receptivity vectors, as well as for marketing based on the influence vectors.

1 Introduction

The spread of information in online media or social networks, as well as diseases in physical networks are examples of diffusions or cascades. While it is common to observe the spread of a cascade, the underlying network (i.e., the arcs) are usually unobservable. For example, we can observe when a person falls ill, but we do not know who infected him/her; we can observe when a person buys a product but we do not know whether he/she was influenced by friend’s recommendation or a TV advertisement. In all these settings, we can observe the propagation of information or disease but cannot observe how they propagate.

There has been much work on recovering the underlying latent network based on observational data on cascades. A network is represented by a diffusion matrix which gives the weight/strength of the arcs between all ordered pairs of agents. [21] introduces a continuous time diffusion model, and recovers the underlying network diffusion matrix by maximizing the log likelihood function. The model of [21] does not assume any structure among nodes, and allows for arbitrary diffusion matrices.

[2] considers a more detailed topic-sensitive model where each information cascade is associated with a set of topics, and there is a distinct diffusion matrix for each topic. This

allows one to capture the intuition that news on certain topics (e.g., information technology) usually spread much faster and broader than others (e.g., military). However, the diffusion matrix for each topic can be arbitrary, and does not capture the intuition that nodes have intrinsic topics of interest.

In this paper, we propose a model based on the intuition that the structure of information diffusion networks should incorporate node specific topics of interests. Throughout the paper we use news as example of cascades for illustrative purposes. An item of news is usually focused on one or few topics (e.g., entertainment, foreign policy, health), and is more likely to spread between two nodes if both are interested in these same topics. Further, it is more likely to spread from node 1 to node 2 if node 1 is more influential/authoritative in the topic, and node 2 is more receptive/susceptible to the topic. In this paper we provide a mathematical model capturing this intuition. We show how to recover the node-topic structure (influence and receptivity) based on observed cascades. This structure can then be used to predict future diffusions, or for customer segmentation based on interests. Finally, after obtaining such a network structure, we can then use it to assign a topic weight vector to a new cascade. For example, an unknown disease can be classified by looking at its propagation behavior.

To the best of our knowledge this is the first paper to incorporate users' interests for estimating the underlying network structure from cascades. Through experiments we illustrate scalability of our model to large networks and robustness to overfitting, while having better interpretability. Our novel models allows us to provide the topic interest distribution for each node, rather than large graph of network structure as is common in existing literature. The results can be used to build recommendation systems, and also for marketing like targeted advertising, which are impossible for existing works.

1.1 Related Work

There is a vast literature on modeling of diffusions, network structure recovery, and latent source identification – in the interest of space we cite the ones most relevant to our work. [20] introduced a discrete time Generalized Linear Cascade Model. In the present paper, we focus on network inference under the continuous-time diffusion model introduced in [21], where the authors propose an algorithm (**NetRate**) to recover the network diffusion matrix. In a follow-up work, [6] looks at the problem of finding the best K edge graph of the network. They show that this is NP-hard and they develop an **NetInf** algorithm that can find a near-optimal set of K directed edges. [7] considers a dynamic network inference problem, where it is assumed that there is an unobserved dynamic network that changes over time and proposes **InfoPath** algorithm to recover this dynamic network. [3] relaxes the restriction that the transmission function should have a specific form, and proposes **KernelCascade** algorithm. Unlike the previous algorithms, this algorithm can infer the transmission function automatically from the data. It allows each pair of nodes to have a different type of transmission model and hence better captures the heterogeneous influence among nodes. [22] uses multi-dimensional Hawkes processes to capture the temporal patterns of nodes behaviors. By optimizing nuclear norm and L_1 norm simultaneously, an algorithm **ADM4** recovers the network structure that is both low-rank and sparse. [18] considers external influence in the model: information can reach a node via the links of the social network or through the influence of external sources. [17] further assumes interaction among cascades: competing

cascades decrease each other’s probability of spreading, while cooperating cascades help each other in being adopted throughout the network. [8] proves a lower bound on the number of cascades needed to correctly recover the whole network structure. [10] combines Hawkes processes and topic modeling to simultaneously reason about the information diffusion pathways and the topics of the observed text-based cascades.

The work most closely related to ours is [2], where the basic model of [21] is modified by assuming that cascades with different topics have different diffusion rates. They call it topic-sensitive model and propose **TopicCascade** algorithm. However, this algorithm still fails to account for different interests that nodes may have.

1.2 Organization of the Paper

In Section 2 we briefly review the basic continuous time diffusion network model introduced in [21], and the topic-sensitive model in [2]. Section 3 introduces our node-topic community model for diffusion, and Section 4 gives the optimization algorithm. In Section 5 we discuss some variants of our model. Sections 6 and 7 present experimental results on synthetic dataset and two real world datasets, respectively.

2 Basic Cascade Model

In this section we briefly review the basic continuous time diffusion model introduced in [21] (Sections 2.1 to 2.4) and the topic-sensitive model of [2] (Section 2.5) which is a modification of that basic model.

2.1 Network structure and cascade generating process

The underlying network is composed of p nodes with edges among them, and is parameterized by a non-negative diffusion matrix $A = \{\alpha_{ji}\}$. The parameter α_{ji} measures the transmission rate from j to i , with larger α_{ji} indicating stronger connection. The absence of $j \rightarrow i$ edge is denoted by $\alpha_{ji} = 0$. We do not consider self infection here so we set $\alpha_{ii} = 0$. The cascade based on this network is generated in the following way. First one of the p nodes is infected as a source node at time 0. At the time a node j is infected, it samples a time at which it infects other nodes it can reach. The transmission time τ_{ji} from node j to i is a random number generated from a density $f(\tau; \alpha_{ji})$ for $\tau \geq 0$ (called the *transmission function/kernel*). A node i is infected the first time one of the nodes which can reach i infects it. At this time, i becomes a new source and begins to infect other nodes by sampling the transmission times to the uninfected nodes.

We assume that our observation window is for T time units since the infection of the source node; nodes that are not infected until time T are regarded as uninfected. We write $f(t_i|t_j; \alpha) = f(t_i - t_j; \alpha_{ji})$ to indicate the density that i is infected by j at time t_i given that j is infected at time t_j , parameterized by α_{ji} . We assume transmission times are independent, and an infected node remains infected in the whole process.

2.2 Data

The observational data consists of n independent cascades denoted by the set C^n , and represented by $\{\mathbf{t}^1, \dots, \mathbf{t}^n\}$. A cascade c is represented by \mathbf{t}^c which is a p -dimensional vector $\mathbf{t}^c = (t_1^c, \dots, t_p^c)$ recording the time of infection of the p nodes; $t_i^c \in [0, T^c] \cup \{\infty\}$ with T^c being the observation window for cascade c . We will assume $T^c = T$ for all cascades, although this assumption is not necessary. If a node is infected by multiple neighbors, only the first infected time is recorded. $t_i^c = 0$ means node i is a source node and $t_i^c = \infty$ means node i is uninfected up to time T .

2.3 Likelihood function

The likelihood function of a cascade \mathbf{t} is

$$f(\mathbf{t}; \mathbf{A}) = \prod_{t_i \leq T} \prod_{t_m > T} S(T|t_i; \alpha_{im}) \times \prod_{k: t_k < t_i} S(t_i|t_k; \alpha_{ki}) \sum_{j: t_j < t_i} H(t_i|t_j; \alpha_{ji}) \quad (1)$$

where $S(t_i|t_j; \alpha_{ji}) = 1 - \int_{t_j}^{t_i} f(t - t_j; \alpha_{ji}) dt$ is the survival function and $H(t_i|t_j; \alpha_{ji}) = f(t_i - t_j; \alpha_{ji})/S(t_i|t_j; \alpha_{ji})$ is the hazard function.

Common transmission functions are exponential, Rayleigh, and power-law distributions [21]. For exponential transmission we have $f(\tau; \alpha_{ji}) = \alpha_{ji} \cdot \exp(-\alpha_{ji}\tau)$ for $\tau \geq 0$ and $f(\tau; \alpha_{ji}) = 0$ otherwise. We then have $S(t + \tau|t; \alpha_{ji}) = \exp(-\alpha_{ji}\tau)$ and $H(t + \tau|t; \alpha_{ji}) = \alpha_{ji}$. Here the diffusion rate reaches its maximum value at the beginning and then decreases exponentially. It can be used to model information diffusion among internet or social network, since (breaking) news usually spread among people immediately. For Rayleigh transmission we have $f(\tau; \alpha_{ji}) = \alpha_{ji}\tau \exp(-\frac{1}{2}\alpha_{ji}\tau^2)$ for $\tau \geq 0$ and $f(\tau; \alpha_{ji}) = 0$ otherwise. We then have $S(t + \tau|t; \alpha_{ji}) = \exp(-\frac{1}{2}\alpha_{ji}\tau^2)$ and $H(t + \tau|t; \alpha_{ji}) = \alpha_{ji}\tau$. Here the diffusion rate is small at the beginning; it then rises to a peak and then drops. It can be used to model citation networks, since it usually takes some time to publish a new paper, and new papers gradually become known by researchers. We are going to use these two transmission functions in Section 7 on the two real datasets.

2.4 Optimization problem

The problem of recovering the unknown diffusion matrix A can be solved by maximum likelihood estimation:

$$\begin{aligned} \text{minimize} \quad & -\frac{1}{n} \sum_{c \in C^n} \log f(\mathbf{t}^c; \mathbf{A}) \\ \text{subject to} \quad & \alpha_{ji} \geq 0, j \neq i \end{aligned} \quad (2)$$

This problem is further separable into p independent subproblems where the i th subproblem is to infer the incoming edges into node i :

$$\begin{aligned} \text{minimize} \quad & \ell^n(\boldsymbol{\alpha}_i) \\ \text{subject to} \quad & \alpha_{ji} \geq 0, j \neq i \end{aligned} \quad (3)$$

Here the parameters $\boldsymbol{\alpha}_i = \{\alpha_{ji} | j = 1, \dots, N, j \neq i\}$ are the relevant variables (the i^{th} column of \mathbf{A}), $\ell^n(\boldsymbol{\alpha}_i) = -\frac{1}{n} \sum_{c \in C^n} g_i(\mathbf{t}^c; \boldsymbol{\alpha}_i)$, and $g_i(\cdot; \boldsymbol{\alpha}_i)$ is the likelihood function for one cascade. For example, for an exponential transmission function, we have

$$g_i(\mathbf{t}; \boldsymbol{\alpha}_i) = \log \left(\sum_{j: t_j < t_i} \alpha_{ji} \right) - \sum_{j: t_j < t_i} \alpha_{ji} (t_i - t_j) \quad (4)$$

for an infected node, and

$$g_i(\mathbf{t}; \boldsymbol{\alpha}_i) = - \sum_{j: t_j < T} \alpha_{ji} (T - t_j) \quad (5)$$

for an uninfected node. More detailed formula can be found in [21].

The maximum likelihood estimation problem is convex in $\boldsymbol{\alpha}_i$ and therefore eminently tractable. Another good property of the formulation is that the linear terms in $\boldsymbol{\alpha}_i$ in the log-likelihood $g(\cdot; \boldsymbol{\alpha}_i)$ (4)-(5) act as an ‘ L_1 penalty.’ Therefore the maximum likelihood solution automatically prefers a sparse solution. Nonetheless, we can still add L_1 penalty to get better results by solving the regularized optimization problem [8]:

$$\begin{aligned} & \text{minimize} && \ell^n(\boldsymbol{\alpha}_i) + \lambda \|\boldsymbol{\alpha}_i\|_1 \\ & \text{subject to} && \alpha_{ji} \geq 0, j \neq i \end{aligned} \quad (6)$$

The problem remains a convex optimization problem and can be efficiently solved by proximal gradient algorithm [19].

2.5 Topic-sensitive model

The basic model assumes that each cascade spreads based on the same diffusion matrix A which is an unrealistic assumption in practice. For example, posts on information technology usually spread much faster than those of economy and military. In [2] the authors handle this by modifying the basic model to a topic-sensitive model. Specifically, they assume that there are in total K topics, and each cascade can be represented as a topic vector in the canonical K -dimensional simplex, in which each component is the weight of a topic: $\mathbf{m}^c := (m_1^c, \dots, m_K^c)^T$ with $\sum_i m_i^c = 1$ and $m_i^c \in [0, 1]$. Each topic k is assumed to have its own diffusion matrix $A^k = \{\alpha_{ji}^k\}$, and the diffusion matrix of the cascade $A^c = \{\alpha_{ji}^c\}$ is the weighted sum of the K matrices:

$$\alpha_{ji}^c = \sum_{k=1}^K \alpha_{ji}^k m_k^c. \quad (7)$$

Given the cascade diffusion matrix A^c , the propagation model remains the same as the basic model. The authors employ a group lasso type regularization ($\sum_j \|\alpha_{ji}\|_2$) on the parameters and solve the problem of inferring A^1, \dots, A^K by maximizing the regularized log-likelihood function, using block coordinate descent and proximal gradient algorithm. More details can be found in [2].

3 An Influence-Receptivity based Topic-sensitive Diffusion Model

Neither of the two models discussed in Section 2 require any structural assumptions on A or A^k other than nonnegativity and sparsity. We posit that there is in fact some structural regularity in the diffusion network. For example, different social media outlets usually focus on different topics, like information technology, economy or military. If the main focus of a media outlet is information technology, then it is more likely to publish or cite news with that topic. Here the topics of interest of a media outlet imparts the network structure. In a university, students may be interested in different academic subjects, may have different music preferences, or follow different sports. Therefore, students who share the same or similar areas of interest may have much stronger connections. Here the areas of interest among students impart the structure. In the context of epidemiology, people usually have different immune systems, and a disease such as flu, usually tends to infect some specific people, while leaving others uninfected. The infected people may have similar immune system, and hence are more likely to become contagious together. Here the types of immune system among people imparts structure to the diffusion network.

To incorporate the above, we modify the topic-sensitive diffusion model of [2] by imposing further structural assumptions on the cascade diffusion matrix A^c . Throughout the paper we use the diffusion of news among people and media outlets as an example of a cascade. As before, our network is composed of p nodes. A cascade c is represented by its weight on K potential topics ($K \ll p$): $\mathbf{m}^c = (m_1^c, m_2^c, \dots, m_K^c)^T$, with $\sum_i m_i^c = 1$ and $m_i^c \in [0, 1]$. A node is parameterized by its ‘interest’ in each of these K topics as a K dimensional vector. Therefore the ‘interest’ of all the p nodes will form a $p \times K$ dimension matrix. We propose two node-topic matrices $B_1, B_2 \in \mathbb{R}^{p \times K}$ to describe such structure. B_1 measures how much a node can infect others (the *influence* matrix) and B_2 measures how much a node can be infected by others (the *receptivity* matrix). We use b_{ij}^1 and b_{ij}^2 to denote the elements of B_1 and B_2 , respectively. A large b_{ij}^1 means that node i is very likely to infect others on topic j ; while a large b_{ij}^2 means that node i is very likely to be infected by others on topic j . The reason why we propose two matrices is that, in general, the behavior of infecting others and being infected by others is different for a node. For example a media outlet i may have many experts in a topic area j , hence it will publish many authoritative news articles about this topic which will be well-cited leading to a large b_{ij}^1 . However, its b_{ij}^2 may not be large, because i has experts in topic j and does not cite other news outlets on topic j . On the flip side, if a media i is only interested in topic j but does not have many experts, then it will have a small b_{ij}^1 and a large b_{ij}^2 .

For a cascade c on topic k , there will be an edge $j \rightarrow i$ if and only if node j tends to infect others on topic k (large b_{jk}^1) and node i tends to be infected by others on topic k (large b_{ik}^2). More generally, for a cascade c with topic-weight vector \mathbf{m}^c , the diffusion parameter α_{ji}^c is

$$\alpha_{ji}^c = \sum_{k=1}^K b_{jk}^1 \cdot m_k^c \cdot b_{ik}^2 \quad (8)$$

or in matrix form,

$$A^c = B_1 \cdot M^c \cdot B_2^T \quad (9)$$

where M^c is a diagonal matrix

$$M^c = \begin{pmatrix} m_1^c & & & \\ & m_2^c & & \\ & & \ddots & \\ & & & m_K^c \end{pmatrix} \quad (10)$$

Finally to ensure that the diagonal elements of A^c are 0, we modify (9) to:

$$A^c = B_1 M^c B_2^T - \text{diag}(B_1 M^c B_2^T). \quad (11)$$

We assume that the matrix M^c is known for each cascade $c \in C^n$, so the parameters to be estimated are B_1 and B_2 only. In practice the topic weights \mathbf{m}^c can be calculated by topic modeling [1]. In topic modeling the number of topics K need to be pre-specified to an appropriate number, or alternatively decided by [11] which learns the distribution over the number of topics.

In addition to $b_{ij}^1, b_{ij}^2 \geq 0$ for each i, j we also impose the constraint that the column sums of B_1 and B_2 are equal: $\mathbf{1}^T B_1 = \mathbf{1}^T B_2$ where $\mathbf{1} \in \mathbb{R}^p$ is all 1 column vector. This means that, for each topic k , the total magnitudes of ‘influence’ and ‘receptivity’ are the same. This acts like a conservation law that the total amount of output should be equal to the total amount of input. The need for this constraint is motivated by two reasons. First, scaling the k th column of B^1 by any constant γ and the k th column of B^2 by $1/\gamma$ results in the same cascade diffusion matrix. Enforcing equal column sums allows us to handle this non-identifiability issue. Second, we want rows of B^1 and B^2 to be interpretable as the relative interest of a user on the K topics. A reasonable assumption would be that for each topic k , the ratio of k th column sum of B^1 and k th column sum of B^2 is invariant to the topic. To interpret each row, the precise value of this ratio is immaterial, and the constraint we impose sets this ratio to 1.

Our model has about $2pK$ parameters, which is much smaller than the original model (p^2 parameters) and the topic-sensitive model (p^2K parameters) since we usually have $K \ll p$. In fact our model is a special case of the topic-sensitive model where we constrain each topic diffusion matrix A^k to be rank 1, suggesting a natural generalization by relaxing this rank 1 constraint to higher ranks.

4 Optimization

4.1 Parameter estimation

As we mentioned earlier, for exposition we assume that the transmission function f follows exponential distribution. The log-likelihood function for our model is easily obtained by plugging the expression for A^c (9) into the original problem (2). However, the maximum likelihood estimation problem is not separable so we have to deal with the entire B_1 and B_2

matrices. We impose an L_1 regularization on B_1 and B_2 to encourage sparsity and to get better estimation result. The optimization problem is given in (12)

$$\begin{aligned} \text{minimize} \quad & -\frac{1}{n} \sum_{c \in C^n} \log f(\mathbf{t}^c; A^c) + \lambda \|B_1 + B_2\|_{1,1} \\ \text{subject to} \quad & A^c = B_1 M^c B_2^T \\ & \mathbf{1}^T B_1 = \mathbf{1}^T B_2 \\ & b_{ij}^1, b_{ij}^2 \geq 0, i \neq j \end{aligned} \quad (12)$$

where we use the norm

$$\|B_1 + B_2\|_{1,1} \triangleq \sum_{i,j} b_{ij}^1 + b_{ij}^2.$$

Rather satisfyingly, the column sum constraint $\mathbf{1}^T B_1 = \mathbf{1}^T B_2$ is automatically satisfied by solving (12), as long as $\lambda > 0$. To see this property, first notice that if we write $B_1 = [u_1, \dots, u_K]$ and $B_2 = [v_1, \dots, v_K]$ we can rewrite our model (9) as

$$A^c = B_1 M^c B_2^T = \sum_{i=1}^K m_i^c \cdot u_i v_i^T. \quad (13)$$

Therefore, if we multiply column i of B_1 by some scalar γ and multiply column i of B_2 by $1/\gamma$, the matrix A^c remains unchanged for any c , since $u_i v_i^T$ does not change. Hence the log-likelihood function also remains unchanged. To get the minimizer we must use the regularization term. If we focus on column i only, then the term we want to minimize is

$$\gamma \cdot \|u_i\|_1 + \frac{1}{\gamma} \|v_i\|_1 \quad (14)$$

To minimize (14) we should select γ that makes the two terms in (14) to be equal. In other words, the column sums of B_1 and B_2 are equal.

We can then remove this constraint from our optimization problem (12) and get our new problem:

$$\begin{aligned} \text{minimize} \quad & -\frac{1}{n} \sum_{c \in C^n} \log f(\mathbf{t}^c; A^c) + \lambda \|B_1 + B_2\|_{1,1} \\ \text{subject to} \quad & A^c = B_1 M^c B_2^T \\ & b_{ij}^1, b_{ij}^2 \geq 0, i \neq j \end{aligned} \quad (15)$$

4.2 Optimization algorithm

Although f is convex in the diffusion matrix A , the minimization problem (15) is not convex in B_1, B_2 . But since f is convex, the problem is biconvex in B_1 and B_2 , which means that with a fixed B_1 , the problem is convex in B_2 and with a fixed B_2 , the problem is convex in B_1 . There are several methods which address optimization of biconvex functions, see [9] for a survey. In general there is no efficient algorithm that can find the global optima for biconvex optimization. [4] proposed a Global Optimization Algorithm (GOP) by alternatively solving

Algorithm 1 Alternating proximal gradient descent

```
Input:  $M, t, T, \eta, \lambda, \epsilon$ 
Initialize  $B_1, B_2$ 
while tolerance  $> \epsilon$  do
   $B_1 = (B_1 - \eta \cdot \frac{\partial \ell}{\partial B_1} - \lambda \eta)_+$ 
   $B_2 = (B_2 - \eta \cdot \frac{\partial \ell}{\partial B_2} - \lambda \eta)_+$ 
end while
```

primal problem and relaxed dual problem. It is guaranteed to find global optima but in general it needs to solve exponential number of subproblems in each iteration. We choose to use alternating proximal gradient descent to solve the problem.

We start with initial B_1, B_2 and alternatively apply proximal gradient method [19] on B_1 and B_2 until we reach a pre-specified tolerance level ϵ . The overall procedure is given in Algorithm 1. To further accelerate the algorithm, one can instead use stochastic gradient descent, with techniques like momentum or ADAM. This may yield a more scalable solution.

In Algorithm 1, M is the set of topic weights M^c for all cascade c ; t is the set of records of infection time t^c for all cascade c ; T is the maximum observation time; η is step size; λ is regularization parameter; and ϵ is tolerance level; $\ell = -\frac{1}{n} \sum_{c \in C^n} \log f(t^c; A^c)$ is the negative log-likelihood function in (15).

5 Some variants and discussions

5.1 Taking friendship into consideration

Since we have used news and media outlets as our running example so far, we assumed that each node can influence any other node. However, in social networks, a user can only see the news or tweets published by their friends or those it chooses to follow. If two users do not know each other, then even if they are interested in similar topics, they still cannot “infect” each other. Considering this we can modify our model in the following way:

$$A^c = B_1 M^c B_2^T \otimes F \quad (16)$$

where \otimes is element-wise multiplication. $F \in \{0, 1\}^{p \times p}$ is a known matrix indicating whether two nodes are “friend” ($f_{ji} = 1$) or not ($f_{ji} = 0$). The modified optimization problem is straightforward extension of (15) by replacing the expression for A^c with the new model (16). The alternating minimization algorithm remains unchanged except for the gradient calculation.

5.2 Estimating topic-weight m^c

Up to now we assume that each M^c is known and we use it to infer the unknown network structure. However, once B_1, B_2 have been estimated, we can use them to classify a new cascade c by recovering its topic-weight vector m^c . For example, if an unknown disease becomes prevalent among people, then we may be able to determine the type of this new disease and the vulnerable population.

The maximum likelihood optimization problem for estimating \mathbf{m}^c is:

$$\begin{aligned} & \text{minimize} && -\log f(\mathbf{t}^c; B_1 M^c B_2^T) \\ & \text{subject to} && \sum_i m_i^c = 1 \\ & && 0 \leq m_i^c \leq 1 \end{aligned} \tag{17}$$

This problem is much easier than (15) since $A^c = B_1 M^c B_2^T$ is linear in M^c , and hence the problem is convex in M^c . The constraint $\sum_{i=1} m_i = 1$ can be incorporated in a projected gradient method to estimate M^c .

5.3 Using node-topic matrices B_1 and B_2

While throughout the paper we use the diffusion of news as the example, our model and the notion of ‘topic’ can be much more general. As shown before it can represent features capturing susceptibility to diseases; as well as geographic position, nationality, etc. Therefore our model can be broadly applied to many areas.

In addition to the ability to forecast future information cascades, the influence-receptivity matrices B_1 and B_2 can also find other uses. For example, we can use the rows of B_2 to learn about the interests of users and for customer segmentation. The rows of B_1, B_2 also act as a natural embedding of users in \mathbb{R}^{2K} and thus defines a similarity metric which can be used in building recommender systems. In epidemiology, we can learn about the vulnerability of population to different diseases, and allocate resources accordingly.

6 Synthetic Datasets

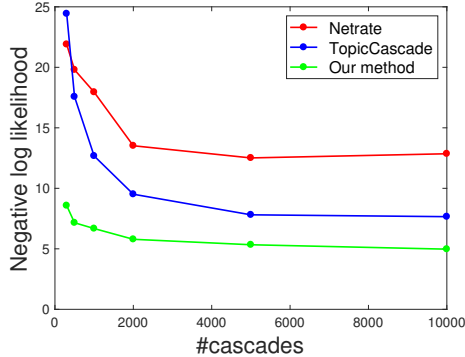


Figure 1: Negative log-likelihood on test dataset

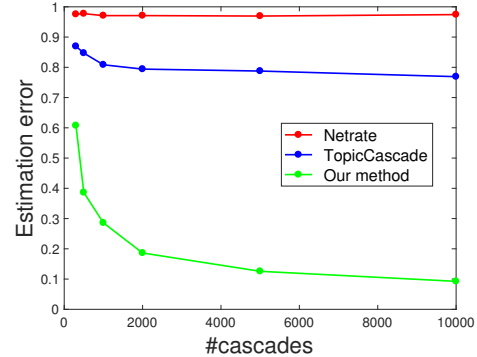


Figure 2: Estimation error

6.1 Estimation accuracy

We first evaluate our model on a synthetic dataset and compare the predictive power of the estimated model with that of Netrate and TopicCascade. In simulation we set $p = 200$ nodes, $K = 10$ topics. We generate the true matrices B_1 and B_2 row by row. For each row, we randomly pick 2-3 topics and assign a random number $\text{Unif}(0.8, 1.8) \cdot \zeta$, where $\zeta = 3$ with probability 0.3 and $\zeta = 1$ with probability 0.7. We make 30% of the values 3 times larger to capture the large variability in interests. All other values are set to be 0 and we scale B_1 and B_2 to have the same column sum. To generate cascades, we randomly choose a node j as the source. The j^{th} row of B_1 describes the “topic distribution” of node j on infecting others. Therefore we sample a K dimensional topic distribution \mathbf{m}^c from $\text{Dir}(b_{j,:}^1)$, where $b_{j,:}^1$ is the j^{th} row of B_1 and $\text{Dir}(\cdot)$ is Dirichlet distribution. According to our model (9), the diffusion matrix of this cascade is $A^c = B_1 M^c B_2^T$. The rest of the cascade propagation follows the description in Section 2. The diffusion process continues until either the overall time exceeds the observation window T , or there are no nodes reachable from the currently infected nodes. We record the first infection time for each node.

We vary the number of cascades $n \in \{300, 500, 1000, 2000, 5000, 10000\}$. For all three models, we fit the model on a training dataset and choose the regularization parameter λ on a validation dataset. Each setting of n is repeated 5 times and we report the average value. We consider two metrics to compare our model with NetRate [21] and TopicCascade [2]:

(1) We generate independent $n = 5000$ test data and calculate negative log-likelihood function on test data for the three models. A good model should be able to generalize well and hence should have small negative log-likelihood. From Figure 1 we see that, when the sample size is small, both Netrate and TopicCascade have large negative log-likelihood on test dataset; while our model generalizes much better. When sample size increases, NetRate still has large negative log-likelihood because it fails to consider the topic structure; TopicCascade behaves more and more closer to our model, which is as expected, since our model is a special case of the the topic-sensitive model. However, our model requires substantially fewer parameters.

(2) We calculate the true diffusion matrix A^k for each topic k based on our model: $A^k = B_1 M_{(k)} B_2^T$ where $M_{(k)}$ is diagonal matrix with 0 on all diagonal elements but 1 on location k . We also generate the estimated \hat{A}^k from the three models as follows: for our model we use the estimated \hat{B}_1 and \hat{B}_2 ; for TopicCascade model the \hat{A}^k is estimated directly as a parameter of the mode; for Netrate we use the estimated \hat{A} as the common topic diffusion matrix for each topic k . Finally, we compare the estimation error of the three models: $\text{error} = \frac{1}{K} \sum_{k=1}^K \frac{\|\hat{A}^k - A^k\|}{\|A^k\|}$. From Figure 2 we see that both Netrate and TopicCascade have large estimation error even if we have many samples; while our model has much smaller estimation error.

6.2 Running time

We then compare the running time of the three methods. For fair comparison, for each method we set the step size, initialization, penalty λ , and tolerance level to be the same. Also one third of the samples are generated by each model, and for the samples generating from Netrate, we randomly assign topic distributions. We run the three method on 12 kernels.

Table 1: Running time comparison

	$\xi = 1$	$\xi = 2$	$\xi = 5$	$\xi = 8$
Netrate	1.15	4.42	53.52	211.0
TopicCascade	5.43	36.10	153.03	1310.7
Our method	9.79	19.83	91.95	454.9

For Netrate and TopicCascade, since they are separable in each column, we run 12 columns in parallel; for our method, we calculate the gradient in parallel. We use our Algorithm 1 for our method and the proximal gradient algorithm for the other two methods, as suggested in [8]. We fix a baseline model size $n = 500, p = 50, K = 10$, and set a free parameter ξ . For $\xi = \{1, 2, 5, 8\}$, each time we increase n, p by a factor of ξ and record the running time (in seconds) of each method. Table 1 summarizes the results based on 5 replications in each setting. We can see that Netrate is the fastest because it does not consider the topics distribution. When p becomes large, our algorithm is faster than TopicCascade and is of the same order with Netrate. This demonstrates that although our model is not separable in each column, it can still deal with large network.

7 Real World Dataset

In this section we evaluate our model on two real world datasets.

7.1 Memetracker Dataset

The first dataset is the MemeTracker dataset [14][12]¹. This dataset contains 172 million news articles and blog posts from 1 million online sources over a period of one year from September 1, 2008 till August 31, 2009. Since the use of hyperlinks to refer to the source of information is relatively rare in mainstream media, the authors use the MemeTracker methodology [15] to extract more than 343 million short textual phrases. After aggregating different textual variants of the same phrase, we consider each phrase cluster as a separate cascade c . Since all documents are time stamped, a cascade c is simply a set of time-stamps when websites first mentioned a phrase in the phrase cluster c . Also since the information diffusion among internet is extremely fast, we use exponential transmission function here.

For our experiments we use the top 500 media sites and blogs with the largest 5000 cascades (phrase clusters). For each website we record the time when they first mention a phrase in the particular phrase cluster. We set the number of topic K to be 10, and perform Topic Modeling to extract 10 most popular topics. We choose the regularization parameter λ on a hold-out validation set, and then use our Algorithm 1 to estimate the two node-topic matrices. The two matrices and the key words of the 10 topics are given in Tables 3 (B_1) and Table 4 (B_2). The keywords of the 10 topics are shown at the head of each table; the first column is the url of the website. The websites above the center line in each table are

¹Data available at <http://www.memetracker.org/data.html>

the most popular websites. We have also hand-picked some less popular websites below the center line whose url suggest that they focus on specific topics, for example politics, business, sports, etc. The top websites are mostly web portals and they broadly post and cite news in many topics. Therefore to demonstrate that our model does extract some meaningful information, we select less popular websites below the center line and hope we can correctly extract the topics of interest of these specific websites.

From the two tables we can see that in general the influence matrix B_1 is much sparser than the receptivity matrix B_2 , which means that websites tend to post news and blogs in many topics but only a few of them will be cited by others. The websites we hand pick are not as active as the top websites. Therefore the values for these websites are much smaller. For the top websites we only display entries which are above the threshold of 0.1, and leave smaller entries blank in the two tables; for the hand selected websites, only 0 values are left blank. From the two tables we see that our model performs quite well on those specific websites. For example the political websites have a large value on topic 4 (election); the business and economics websites have large value on topic 3 (economy), etc. Those “as expected” large values are shown in boldface in order to highlight them.

We then visualize the estimated B_1 and B_2 using t-SNE algorithm [16] to see whether nodes are clustered with respect to a set of topics, and whether the clusters in B_1 correspond to the ones in B_2 . In B_1 and B_2 , each row is a 10 dimensional vector corresponding to a website. We use t-SNE algorithm to give each website a location in a two-dimensional map and the scatter plot of B_1 and B_2 are given in Figure 3 and Figure 4. From the two figures we see that these points do not form clear clusters, which means most of the websites are in general interested in many of the topics and they do not differ too much from each other. We can see clearer clusters in the next example.

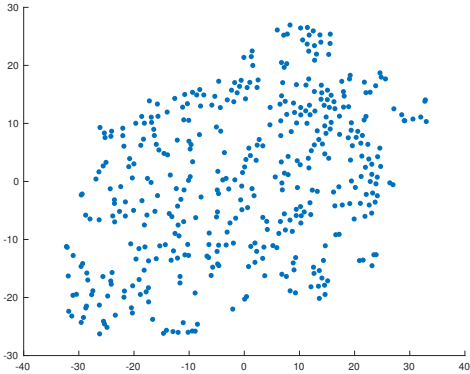


Figure 3: Scatter plot of B_1 using t-SNE algorithm, for Memetracker dataset

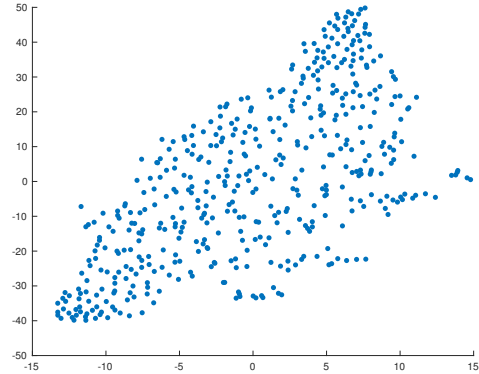


Figure 4: Scatter plot of B_2 using t-SNE algorithm, for Memetracker dataset

Finally we check the performance of our method on about 1500 test cascades and compare with Netrate and TopicCascade. Since the number of parameters are different for the three models, besides negative log-likelihood, we also use AIC and BIC as our metrics. Table 2 summarizes the results. The first column illustrates the names of the three methods and the

Table 2: Comparison of the 3 methods on test cascades for Memetracker dataset

	train	test	para	nonzero	AIC	BIC
Netrate	68.5	81.1	250000	20143	2.60×10^5	3.65×10^5
TopicCascade	62.5	81.8	2500000	142718	5.08×10^5	1.25×10^6
Our method	80.3	82.3	10000	7272	2.38×10^5	2.76×10^5

following columns are the averaged negative log-likelihood on train set, averaged negative log-likelihood on test set, number of total parameters, number of nonzero parameters, AIC and BIC on test set calculated using the negative log-likelihood on test set (third column) and the number of nonzero parameters (fifth column). From the table we see that our model has significantly less parameters than the other two, and hence our model has the largest negative log-likelihood on train set. However, we can see that both Netrate and TopicCascade are clearly overfitting, while our method can generalize to test set with little overfitting. Our method uses much less parameters but has comparable negative log-likelihood on test, and also our method has the smallest AIC and BIC value. So in conclusion, we see that our model works quite well on this Memetracker dataset.

7.2 Arxiv Citation Dataset

The second dataset is the ArXiv high-energy physics theory citation network dataset [13][5]². This dataset includes all papers published in ArXiv high-energy physics theory section from 1992 to 2003. We treat each author as a node and each publication as a cascade. For our experiments we use the top 500 authors with the largest 5000 cascades. For each author we record the time when they first cite a particular paper. Since it usually takes some time to publish papers we use rayleigh transmission function here. We set the number of topic K to be 6, and perform Topic Modeling on the abstracts of each paper to extract 6 most popular topics. We then use our Algorithm 1 to estimate the two node-topic matrices. The two matrices and the key words of the 6 topics are given in Tables 6 (B_1) and Table 7 (B_2). Again the keywords of the 6 topics are shown at the head of each table and the first column is the name of the author.

We compare the learnt topics to the research interests listed by the authors in their website and we find that our model is able to discover the research topics of the authors accurately. For example Arkady Tseytlin reports string theory, quantum field theory and gauge theory; Shin’ichi Nojiri reports field theory; Burt A. Ovrut reports gauge theory; Amihay Hanany reports string theory; Ashoke Sen reports string theory and black holes as their research areas in their webpages. Moreover, Ashok Das has papers in supergravity, supersymmetry, string theory, and algebras; Ian Kogan has papers in string theory and boundary states; Gregory Moore has papers in algebras and non-commutativity. These are all successfully captured by our method.

We then again visualize the estimated B_1 and B_2 using t-SNE algorithm and the scatter

²Data available at <http://snap.stanford.edu/data/cit-HepTh.html>

Table 3: The influence matrix B_1 for Memetracker dataset

	energy	love	market	obama	think	new	people	government	life	time
	power	man	price	mccain	play	technology	clergy	law	world	year
	oil	life	money	president	team	system	food	public	church	student
	gas	time	economy	party	game	data	problem	state	lord	community
blog.myspace.com	0.29	0.17	0.17		0.11	0.25	0.54	0.12	0.24	0.43
us.rd.yahoo.com	0.7	0.33	0.24	0.18	0.15	0.38	0.28	0.4	0.42	0.61
news.google.com	0.15	0.13	0.15		0.13			0.15		0.65
startribune.com	0.42	0.59	0.5	0.3	0.32	0.49		0.24	0.31	
news.com.au						0.12	0.18		0.2	
breitbart.com	0.77	0.47		0.15	0.16	0.37		0.25	0.55	
uk.news.yahoo.com	0.51	0.3	0.36		0.17	0.3	0.33	0.13		0.15
cnn.com	0.13	0.15	0.5	0.19			0.34			0.12
newsmeat.com				0.55						
washingtonpost.com	0.10	0.41	0.14	0.10	0.10	0.39	0.13	0.23	0.22	
forum.prisonplanet.com	0.2								0.17	
news.originalsignal.com		0.13								0.17
c.moreover.com						0.19	0.24			
philly.com										
rss.feedportal.com		0.1	0.14			0.15		0.18		0.19
foxnews.com	0.099	0.17	0.26	0.052	0.071					0.085
sports.espn.go.com		0.038		0.29	0.23		0.12	0.41		
olympics.thestar.com				0.013	0.036					0.012
forbes.com	0.019		0.028		0.02				0.035	
scienceblogs.com	0.24	0.14	0.077	0.2	0.12	0.15	0.092	0.052	0.29	0.091
swamppolitics.com				0.42	0.049					
cqpolitics.com	0.016	0.23	0.082	0.16	0.23				0.045	

Table 4: The receptivity matrix B_2 for Memetracker dataset

	energy	love	market	obama	think	new	people	government	life	time
	power	man	price	mccain	play	technology	clergy	law	world	year
	oil	life	money	president	team	system	food	public	church	student
	gas	time	economy	party	game	data	problem	state	lord	community
blog.myspace.com	0.42	0.63	0.28	0.47	0.55	0.18	0.29	0.43	0.49	0.22
us.rd.yahoo.com	0.36	0.28	0.28	0.44	0.56	0.19	0.22	0.41	0.27	0.18
news.google.com	0.15		0.10	0.17				0.12	0.11	
startribune.com	0.19	0.25	0.16	0.37	0.38	0.13	0.14	0.27	0.23	0.13
news.com.au		0.10		0.13	0.12					
breitbart.com	0.14	0.13	0.14	0.3	0.2			0.16	0.18	
uk.news.yahoo.com	0.12	0.14	0.15	0.21	0.14		0.14	0.14	0.13	
cnn.com	0.12	0.15		0.18	0.16			0.15	0.12	
newsmeat.com										
washingtonpost.com	0.12	0.15	0.15	0.23	0.17	0.12	0.1	0.16	0.18	
forum.prisonplanet.com					0.10				0.10	
news.originalsignal.com	0.22	0.23	0.18	0.37	0.26		0.18	0.26	0.21	
c.moreover.com	0.24	0.21	0.15	0.37	0.36	0.11	0.15	0.34	0.25	0.17
philly.com	0.11	0.15		0.16	0.21			0.14	0.11	0.1
rss.feedspotal.com		0.11		0.11		0.1			0.10	
canadianbusiness.com	0.012		0.061			0.017	0.012	0.012		
olympics.thestar.com		0.013			0.023			0.02	0.013	
tech.originalsignal.com	0.036	0.032	0.04	0.031	0.038	0.13	0.037	0.037	0.043	0.031
businessweek.com	0.017		0.032	0.012	0.01	0.015	0.012	0.012	0.017	
economy-finance.com	0.026	0.014	0.072	0.024	0.027	0.036		0.03	0.02	
military.com		0.014		0.037	0.014			0.02	0.014	0.013
security.itworld.com						0.042				0.015
money.canoe.ca	0.011		0.022			0.02		0.012		
computerworld.com	0.011					0.053				

Table 5: Comparison of the 3 methods on test cascades for citation dataset

	train	test	para	nonzero	AIC	BIC
Netrate	66.8	83.9	250000	13793	2.34×10^5	3.05×10^5
TopicCascade	67.3	85.3	1500000	57052	3.24×10^5	6.16×10^5
Our method	78.2	82.3	6000	3738	2.10×10^5	2.29×10^5

plot of B_1 and B_2 are given in Figure 5 and Figure 6. Here we see clear clusters in the two figures. Figure 5 clearly shows 6 “petals” corresponding to the authors interested in 6 topics, while the points in the center corresponds to the authors who have small influence on all the 6 topics. We therefore apply K-Means algorithm to get 7 clusters for the influence matrix B_1 as shown in Figure 5 (each color corresponds to one cluster), and then plot receptivity matrix B_2 in Figure 6 using these colors. We see that although Figure 6 also shows several clusters, the patterns are clearly different from Figure 5. This demonstrates the necessity of having different influence matrix B_1 and receptivity matrix B_2 in our model.

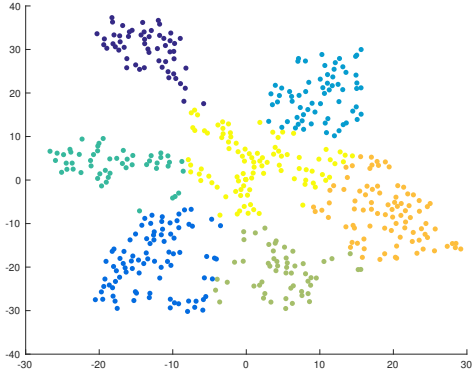


Figure 5: Scatter plot of B_1 using t-SNE algorithm, for Citation dataset

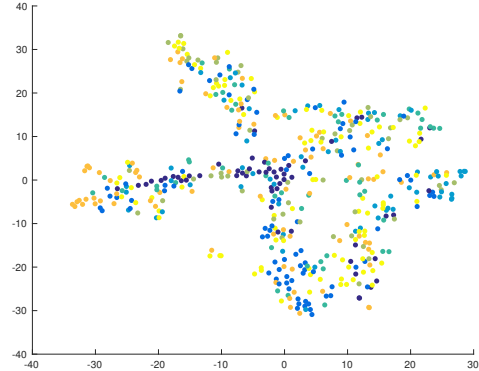


Figure 6: Scatter plot of B_2 using t-SNE algorithm, for Citation dataset

Finally we check the performance of our method on about 1200 test cascades and compare with Netrate and TopicCascade. Table 5 summarizes the results. Similar as before, although Netrate and TopicCascade have smaller negative log-likelihood on train data, our method has the best performance on test data with significantly less parameters and little overfitting. So again we see that our model works quite well on this citation dataset.

8 Conclusion

The majority of work on information diffusion has focused on recovering the diffusion matrix but ignoring the structure among nodes. In this paper we propose an Influence-Receptivity model that takes the structure among nodes into consideration. We develop an efficient

Table 6: The influence matrix B_1 for citation dataset

	black hole energy chains	quantum model field theory	gauge theory field effective	algebra space group structure	states space noncommutative boundary	string theory supergravity supersymmetric
Christopher N. Pope	0.15	0.16	0.062	0.12		
Hong Lu	0.11	0.16	0.067	0.12		
Arkady Tseytlin	0.019	0.37	0.13	0.08		0.18
Sergei D. Odintsov		0.042	0.29		0.037	0.013
Shin'ichi Nojiri		0.028	0.22			
Emilio Elizalde	0.012	0.023	0.11		0.14	
Cumrun Vafa		0.17		0.43		
Edward Witten	0.034	0.019		0.3	0.39	0.036
Ashok Das	0.065	0.018		0.038		0.14
Sergio Ferrara	0.41	0.056		0.2	0.11	
Renata Kallosh	0.16	0.49	0.17	0.11	0.029	
Mirjam Cvetic		0.35	0.04	0.032		0.026
Burt A. Ovrut		0.11	0.23	0.083		
Ergin Sezgin	0.16	0.25	0.54			
Ian Kogan	0.013				0.14	0.11
Gregory Moore				0.04	0.18	
I. Antoniadis	0.21	0.084	0.13	0.32	0.07	0.22
Andrew Strominger		0.37		0.2		
Barton Zwiebach	0.027		0.015	0.15	0.2	
Paul Townsend	0.036	0.72	0.65	0.21		
Robert Myers		0.075	0.023	0.018		
Eric Bergshoeff	0.096	0.062	0.12	0.092		
Amihay Hanany				0.16	0.049	0.22
Ashoke Sen	0.11	0.15		0.48		0.22

Table 7: The receptivity matrix B_2 for citation dataset

	black hole energy chains	quantum model field theory	gauge theory field effective	algebra space group structure	states space noncommutative boundary	string theory supergravity supersymmetric
Christopher N. Pope	0.5	0.78	0.062	0.26		
Hong Lu	0.47	0.86	0.045	0.25		
Arkady Tseytlin	0.23	0.88	0.55	0.3	0.26	
Sergei D. Odintsov		0.58	0.80	0.029	0.14	0.16
Shin'ichi Nojiri		0.29	0.35	0.021		0.17
Emilio Elizalde		0.037	0.18		0.24	0.019
Cumrun Vafa	0.098			0.64	0.087	0.16
Edward Witten	0.097		0.29	0.41	0.28	0.2
Ashok Das	0.2	0.099	0.11	0.023		0.14
Sergio Ferrara	0.51	0.3	0.041	0.53	0.13	
Renata Kallosh	0.19	0.3	0.58	0.16		
Mirjam Cvetic	0.029	1.4	0.077	0.31		0.095
Burt A. Ovrut	0.021	0.17	0.34	0.13		0.12
Ergin Sezgin	0.17	0.062	0.38	0.1		
Ian Kogan	0.061	0.3		0.05	0.42	0.13
Gregory Moore	0.27	0.064	0.28	0.51	0.38	0.056
I. Antoniadis	0.1	0.024	0.042	0.23		0.1
Andrew Strominger	0.032	0.58	0.078	0.1	0.079	
Barton Zwiebach	0.14		0.018	0.096	0.021	0.068
Paul Townsend	0.06	0.12	0.42	0.21		
Robert Myers		0.86	0.2	0.23	0.042	0.04
Eric Bergshoeff	0.24	0.15	0.82	0.27	0.011	
Amihay Hanany				0.65	0.02	0.22
Ashoke Sen		0.057		0.16	0.051	0.04

algorithm and demonstrate experimentally that our model performs well in both synthetic data and real data. Our model has broad application including recommendation system, disease control, and targeted advertisement.

There are several interesting research threads we plan to pursue. Computationally, maximum likelihood estimation for our model is not separable into subproblems as [2]. Exploring computationally scalable estimation algorithms is one of the threads. We would also like to establish convergence properties of our algorithm to local optimal, and whether clever initialization schemes can guarantee global optima in the regime where n is sufficiently large. In terms of modeling, an interesting future direction would be to allow each cascade to have a different propagation rate. In our current model, two cascades with the same topic distribution will have the same diffusion behavior. In real world, we expect some information to be interestingly more interesting and hence spread much faster. Other extensions would be allowing dynamic Influence-Receptivity matrices over time, and also jointly estimating Influence-Receptivity matrices for each node and topic distribution for each cascade. Finally, all existing work on network structure recovery from cascades assumes that the first node observed to be infected is the source of the diffusion. In many scenarios, the source may be latent and directly infect many nodes. Extending our model to incorporate this feature is work in progress.

Acknowledgments

This work is partially supported by an IBM Corporation Faculty Research Fund at the University of Chicago Booth School of Business. This work was completed in part with resources provided by the University of Chicago Research Computing Center.

References

- [1] David M Blei, Andrew Y Ng, and Michael I Jordan. Latent dirichlet allocation. *Journal of machine Learning research*, 3(Jan):993–1022, 2003.
- [2] Nan Du, Le Song, Hyenkyun Woo, and Hongyuan Zha. Uncover topic-sensitive information diffusion networks. In *Proceedings of the sixteenth international conference on artificial intelligence and statistics*, pages 229–237, 2013.
- [3] Nan Du, Le Song, Ming Yuan, and Alex J Smola. Learning networks of heterogeneous influence. In *Advances in Neural Information Processing Systems*, pages 2780–2788, 2012.
- [4] Christodoulos A Floudas. *Deterministic global optimization: theory, methods and applications*, volume 37. Springer Science & Business Media, 2013.
- [5] Johannes Gehrke, Paul Ginsparg, and Jon Kleinberg. Overview of the 2003 kdd cup. *ACM SIGKDD Explorations Newsletter*, 5(2):149–151, 2003.

- [6] Manuel Gomez Rodriguez, Jure Leskovec, and Andreas Krause. Inferring networks of diffusion and influence. In *Proceedings of the 16th ACM SIGKDD international conference on Knowledge discovery and data mining*, pages 1019–1028. ACM, 2010.
- [7] Manuel Gomez Rodriguez, Jure Leskovec, and Bernhard Schölkopf. Structure and dynamics of information pathways in online media. In *Proceedings of the sixth ACM international conference on Web search and data mining*, pages 23–32. ACM, 2013.
- [8] Manuel Gomez-Rodriguez, Le Song, Hadi Daneshmand, and Bernhard Schölkopf. Estimating diffusion networks: Recovery conditions, sample complexity & soft-thresholding algorithm. *Journal of Machine Learning Research*, 2015.
- [9] Jochen Gorski, Frank Pfeuffer, and Kathrin Klamroth. Biconvex sets and optimization with biconvex functions: a survey and extensions. *Mathematical Methods of Operations Research*, 66(3):373–407, 2007.
- [10] Xinran He, Theodoros Rekatsinas, James R Foulds, Lise Getoor, and Yan Liu. Hawkestopic: A joint model for network inference and topic modeling from text-based cascades. In *ICML*, pages 871–880, 2015.
- [11] Wei-Shou Hsu and Pascal Poupart. Online bayesian moment matching for topic modeling with unknown number of topics. In *Advances in Neural Information Processing Systems*, pages 4536–4544, 2016.
- [12] Jure Leskovec, Lars Backstrom, and Jon Kleinberg. Meme-tracking and the dynamics of the news cycle. In *Proceedings of the 15th ACM SIGKDD international conference on Knowledge discovery and data mining*, pages 497–506. ACM, 2009.
- [13] Jure Leskovec, Jon Kleinberg, and Christos Faloutsos. Graphs over time: densification laws, shrinking diameters and possible explanations. In *Proceedings of the eleventh ACM SIGKDD international conference on Knowledge discovery in data mining*, pages 177–187. ACM, 2005.
- [14] Jure Leskovec and Andrej Krevl. SNAP Datasets: Stanford large network dataset collection. <http://snap.stanford.edu/data>, June 2014.
- [15] Jure Leskovec and Rok Sosić. Snap: A general-purpose network analysis and graph-mining library. *ACM Transactions on Intelligent Systems and Technology (TIST)*, 8(1):1, 2016.
- [16] Laurens van der Maaten and Geoffrey Hinton. Visualizing data using t-sne. *Journal of Machine Learning Research*, 9(Nov):2579–2605, 2008.
- [17] Seth A Myers and Jure Leskovec. Clash of the contagions: Cooperation and competition in information diffusion. In *Data Mining (ICDM), 2012 IEEE 12th International Conference on*, pages 539–548. IEEE, 2012.

- [18] Seth A Myers, Chenguang Zhu, and Jure Leskovec. Information diffusion and external influence in networks. In *Proceedings of the 18th ACM SIGKDD international conference on Knowledge discovery and data mining*, pages 33–41. ACM, 2012.
- [19] Neal Parikh and Stephen Boyd. Proximal algorithms. *Foundations and Trends® in Optimization*, 1(3):127–239, 2014.
- [20] Jean Pouget-Abadie and Thibaut Horel. Inferring graphs from cascades: A sparse recovery framework. In *WWW (Companion Volume)*, pages 625–626, 2015.
- [21] Manuel Gomez Rodriguez, David Balduzzi, and Bernhard Schölkopf. Uncovering the temporal dynamics of diffusion networks. *arXiv preprint arXiv:1105.0697*, 2011.
- [22] Ke Zhou, Hongyuan Zha, and Le Song. Learning social infectivity in sparse low-rank networks using multi-dimensional hawkes processes. In *AISTATS*, volume 31, pages 641–649, 2013.